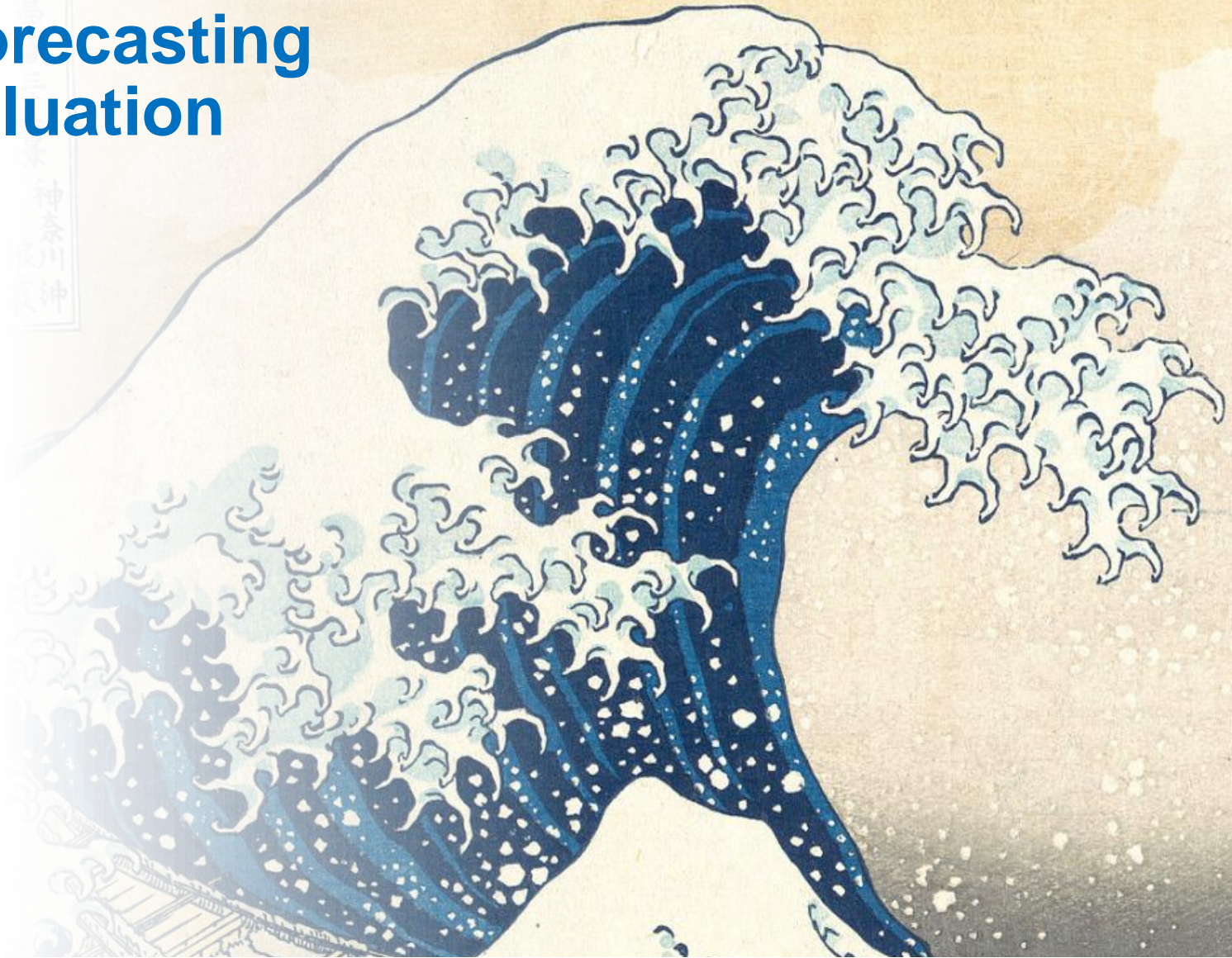


# WP3: Sea State Forecasting and Resource Evaluation

Igor Rizaev, PhD

[i.g.rizaev@hull.ac.uk](mailto:i.g.rizaev@hull.ac.uk)

*Energy and Environment  
Institute, University of Hull*



Engineering and  
Physical Sciences  
Research Council



UNIVERSITY  
OF HULL

ENERGY AND  
ENVIRONMENT INSTITUTE



# SmartWave – High accuracy & high spatial fidelity wave prediction

Motivation: Development of SmartWave to simulate parameters useful for marine renewables.

Artificial Intelligence (Artificial Neural Network – ANN and Convolutional Neural Network – CNN) will be advanced to estimate key oceanographic parameters i.e. wave height, direction, frequency, and speed. State-of-the-art remote sensing monitoring and in situ data from European Space Agency satellite Sentinel 1 (Synthetic Aperture Radar – SAR) will be utilised, whilst access to high-fidelity data from the Cefas WaveNet buoys will provide ground truth data for validation.



# Satellite SAR images

Satellite images are capable of providing hindcast information in very high resolution

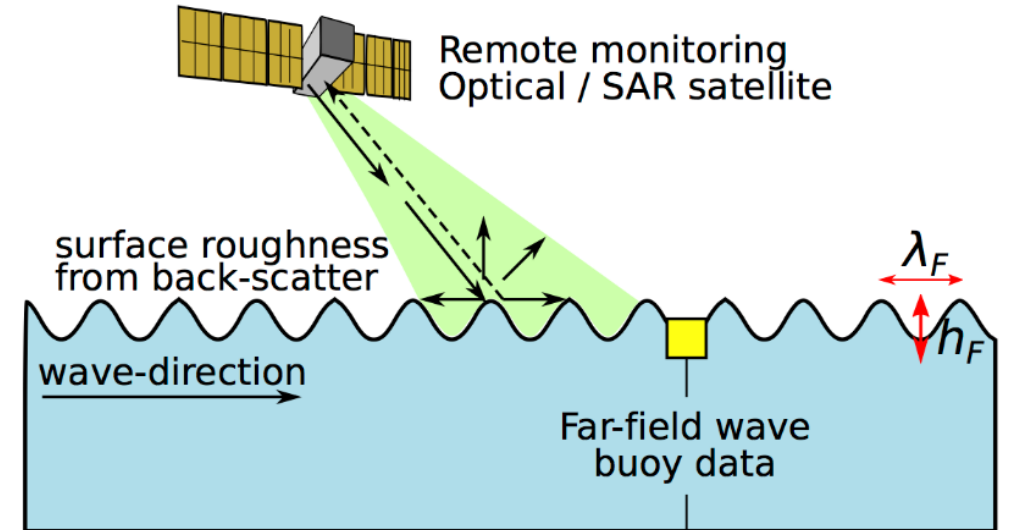
How it works:

- Radar transmits a pulse
- Some of the energy in the radar pulse is reflected back
- Every pixel of a complex SAR image contains amplitude and phase information.

Can provide information about the sea roughness

Using SAR images has benefits:

- Unaffected by weather
- Unaffected by cloud cover
- Larger datasets



# How it works

ANN based system

## Data Acquisition

- Sentinel 1 - SAR Images
- Buoy data

## Data processing

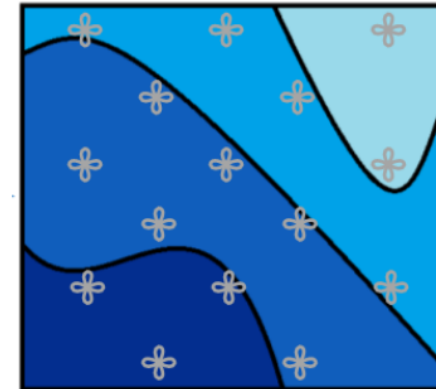
Initial processing,  
Extract parameters related to  
sea roughness from  
different SAR image bands

## Artificial neural networks (ANNs)

Correlate sea roughness  
parameters to buoy data

## Spatial distribution

Apply ANNs to derive  
sea state in any location



# Example results – Burbo Bank

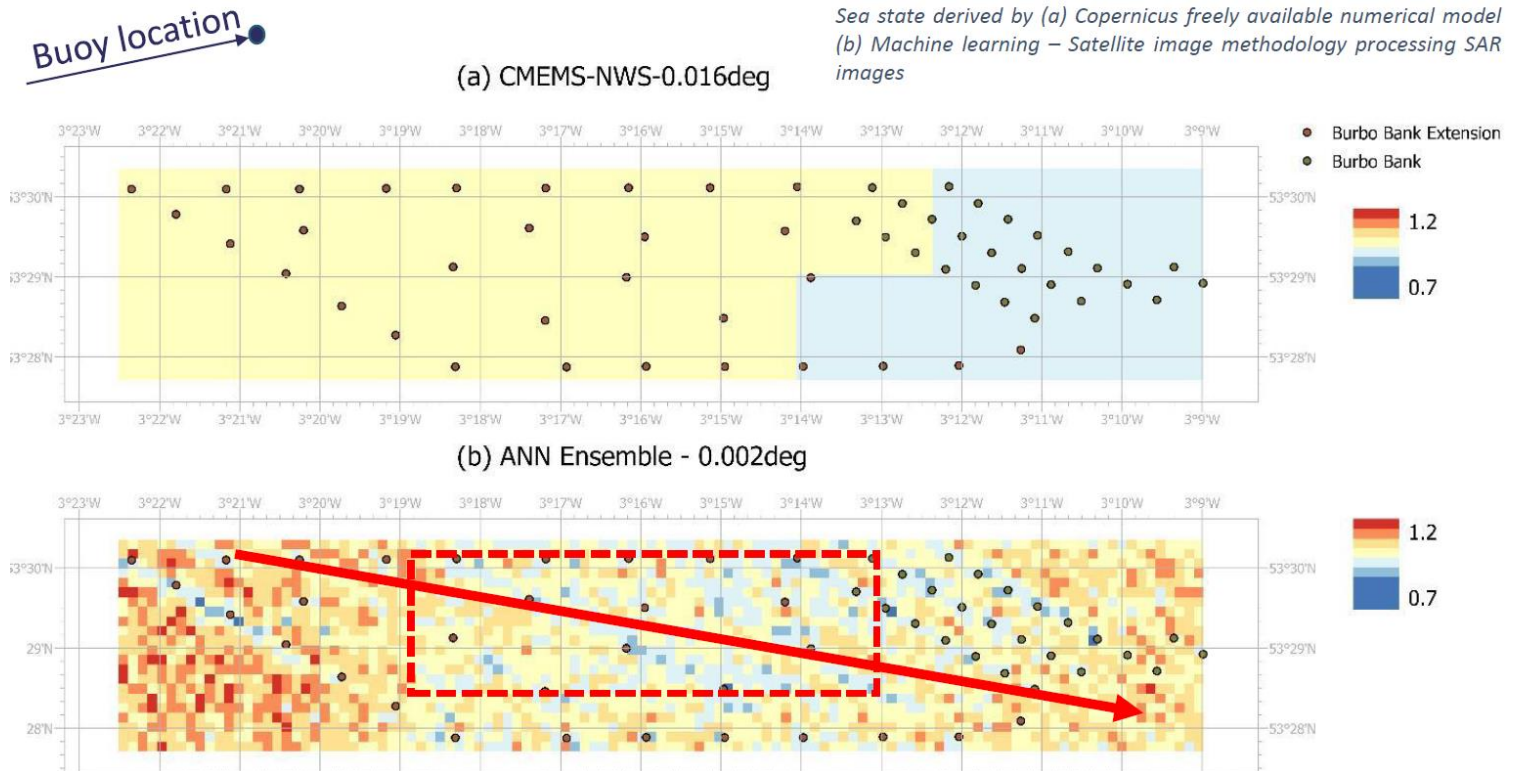
Comparison of Sea state conditions at 2/4/2019 06:32:16am

Buoy data: 0.89m (6:30am) – 1.07m (7:00am)

Numerical model at the buoy: 0.92m

ANN Ensemble: 0.95m

- Same trend of significant wave height for both hindcasts
- Higher resolution for machine learning-satellite image methodology
- Possible to identify patterns like sheltering in the inner wind turbines compared to the ones that are at the edge of the wind farm.



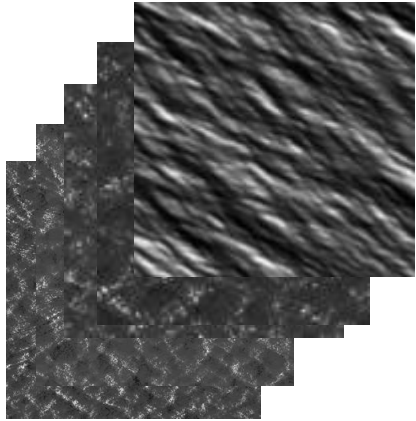
Tapoglou, E., Forster, R. M., Dorrell, R. M., & Parsons, D. (2021). Machine learning for satellite-based sea-state prediction in an offshore windfarm. *Ocean Engineering*, 235, 109280.

# CNN based system

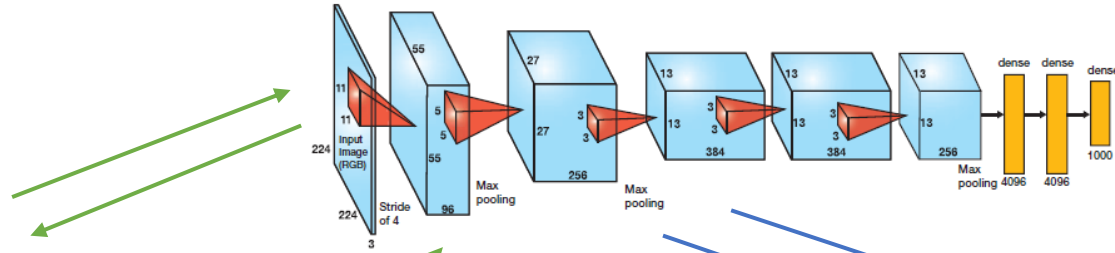
## Deep learning

### SAR imagery synthetic database creation

- Different parameters:
- wind directions
- wind speeds
- fetch size
- incidence angles
- polarizations



### Training CNN (AlexNet)

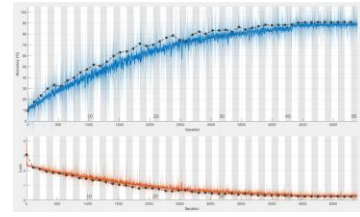


### Strategies:

- Training from scratch
- Transfer learning with real data

- Automated classification and estimation of sea state parameters:
- wave height
- direction
- frequency
- speed

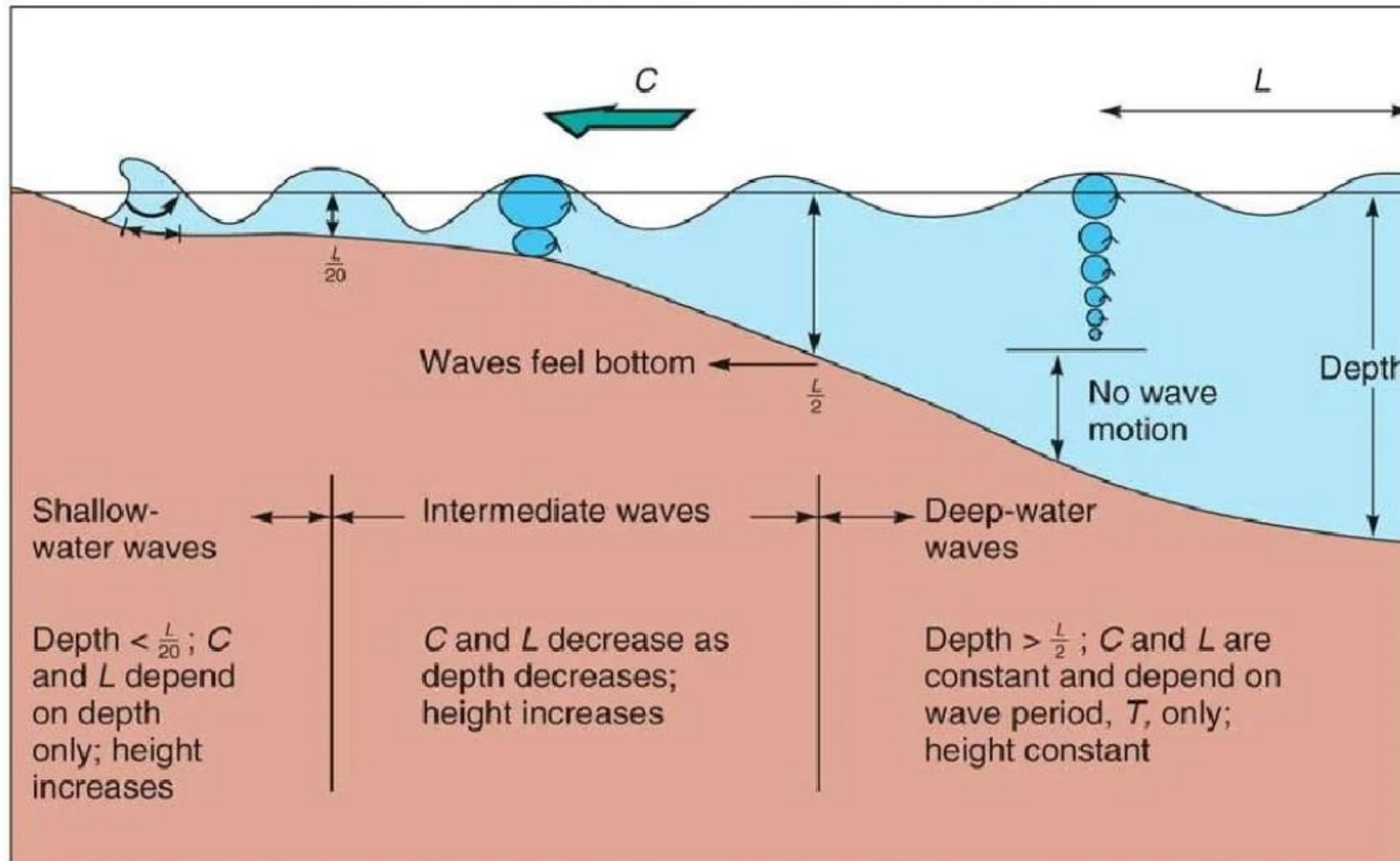
Iter	Eval	objective	objective	BestSoFar	BestSoFar	InitialLearn	momentum	L2Regulariza
result	runtime	(observed)	(estim.)	rate				
1	Best	3	3385.3	1	0.024555	0.43595	0.9777e-08	
2	Best	0.48836	3383.2	0.48836	0.48836	0.5450e-05	0.14615e-08	
3	Accept	0.45364	3384.1	0.48836	0.48836	0.006379	0.12134	2.651e-09
4	Accept	3	3074.6	0.48836	0.48836	0.009715	0.04202	0.000709
5	Accept	0.8931	3124.9	0.48836	0.48836	1.0006e-05	0.54542	2.7270e-10
6	Accept	0.5586	3386.5	0.48836	0.48836	0.002163	0.53962	0.00095463
7	Accept	0.5797	3386.9	0.48836	0.48836	0.003955	0.58886	1.1770e-10
8	Best	0.85932	3385.1	0.48836	0.48836	0.002192	0.57805	0.001046
9	Best	0.838762	3318.5	0.488762	0.488762	0.004432	0.97996	1.0937e-10
10	Accept	0.004883	3387.5	0.488762	0.488762	0.002918	0.87773	1.2902e-08
11	Accept	0.5682	3383.2	0.488762	0.488762	1.0130e-05	0.97007	1.1726e-10
12	Accept	0.043385	3384.7	0.488762	0.488762	0.001907	0.97933	1.0402e-10
13	Accept	0.047774	3383.3	0.488762	0.488762	0.002278	0.93341	0.0041e-08
14	Accept	0.85088	3381	0.488762	0.488762	0.0003718	0.5782	1.0514e-09
15	Accept	0.8668	3384.4	0.488762	0.488762	0.004424	0.8333	2.7624e-09
16	Accept	0.85095	3381	0.489505	0.489505	0.002141	0.8985	0.0009
17	Accept	0.86537	3382	0.489505	0.489505	0.003911	0.80293	1.7411e-08
18	Accept	0.83828	3380.4	0.489505	0.489505	0.003433	0.88702	0.0047099
19	Accept	0.83922	3382.4	0.489505	0.489505	0.002068	0.87014	1.1716e-10
20	Accept	0.83899	3382.9	0.489505	0.489505	0.0027015	0.96409	0.003842
21	Accept	0.87827	3381.6	0.489505	0.489505	0.003047	0.62307	0.0072111
22	Accept	0.84282	3382.3	0.489505	0.489505	0.003828	0.97863	0.0093593
23	Accept	0.84569	3385.2	0.489505	0.489505	0.002352	0.74856	0.0010573
24	Accept	0.11574	3385.5	0.489505	0.489505	0.003281	0.18648	3.5450e-07
25	Accept	3	3074.4	0.489505	0.489505	0.49079	0.10735	9.3844e-05
26	Accept	0.82562	3387.1	0.489505	0.489505	0.003728	0.97489	5.3037e-08
27	Accept	0.86752	3382	0.489505	0.489505	0.004142	0.48467	0.0004835
28	Accept	0.89531	3384	0.489505	0.489505	0.00548	0.97137	0.0001895
29	Accept	0.236	3387.5	0.489505	0.489505	0.0027018	0.27902	0.0027018
30	Accept	0.84126	3382	0.489505	0.489505	0.004904	0.65601	0.0022381



Bayesian optimization to find optimal network hyperparameters

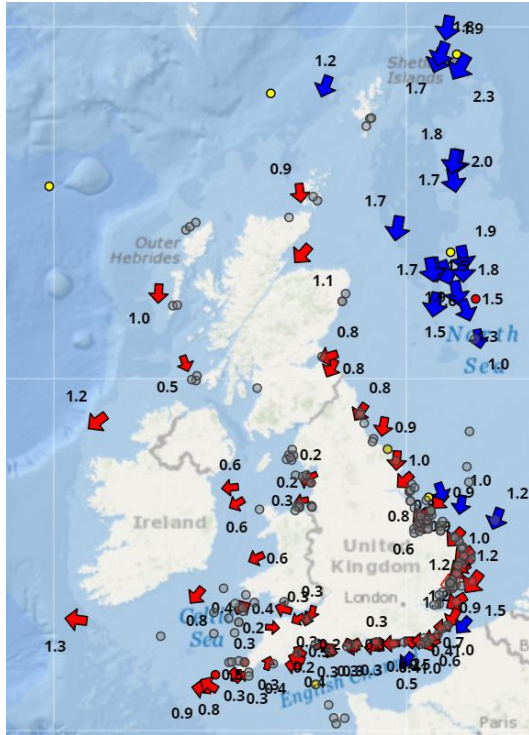


# Relationship between wavelength and water depth

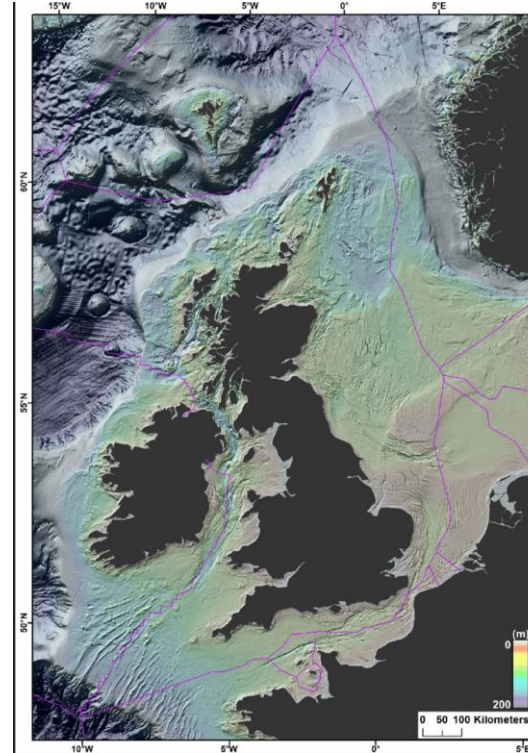


# Mapping of shallow, intermediate, and deep-water areas

Cefas WaveNet buoys



Bathymetry offshore model of the UK (EMODnet and GEBCO)



Determination of uniform waves zones



Dove, D., Bradwell, T., Carter, G., Cotterill, C., Gafeira Goncalves, J., Green, S., ... & Ottesen, D. (2016). Seabed geomorphology: a two-part classification system.



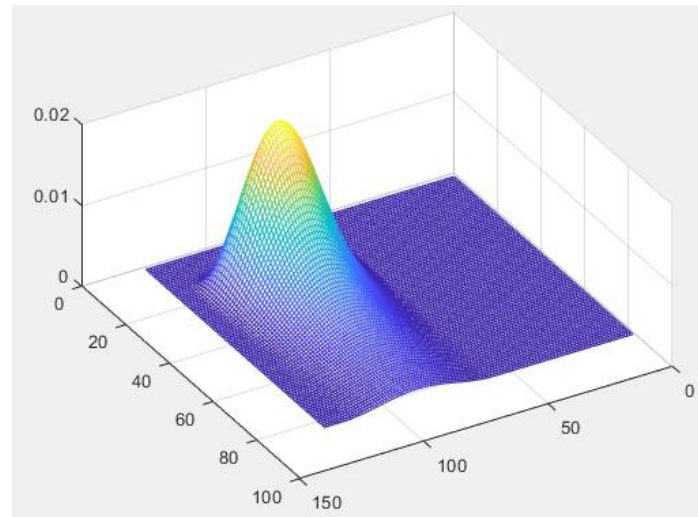
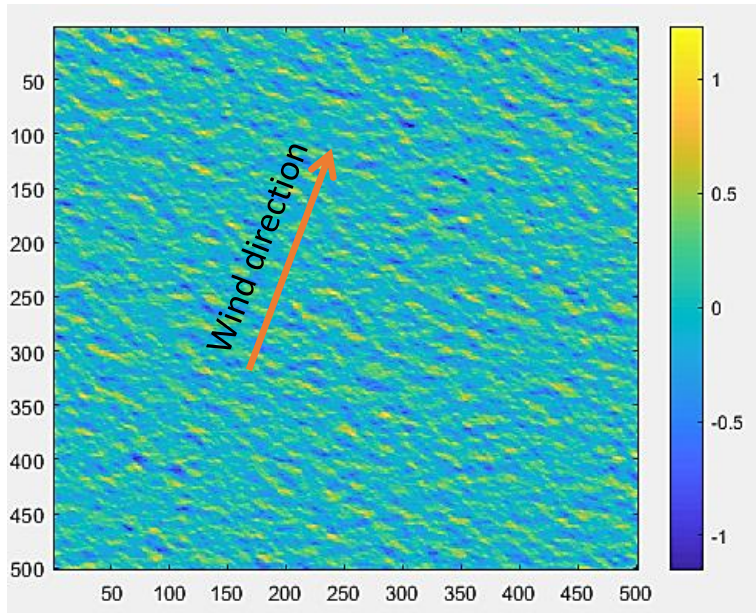
# Sea Surface Modelling - Linear theory

The irregular sea surface elevation model can be expressed as:

$$Z_{sea}(x, y, z, t) = \sum_i \sum_j A_{ij} \cos[k_i(x \cos \theta_j + y \sin \theta_j) - \omega_i t + r_{ij}]$$

Wind speed  $V_w = 7$  m/s

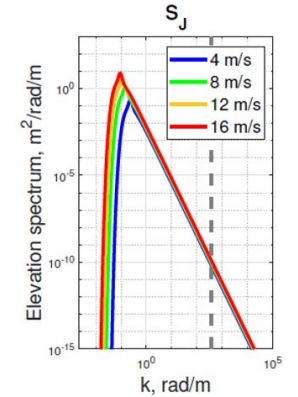
$$A_{ij} = \sqrt{2S(k_i)D(k_i, \theta_j)dk_i d\theta_j}$$



Omnidirectional spectrum

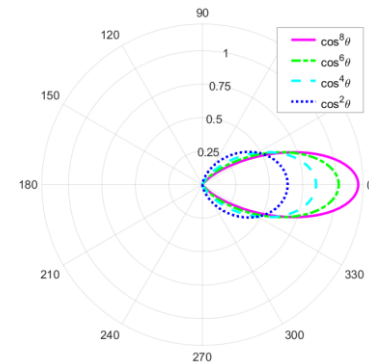
Joint North Sea Wave Project (JONSWAP)

$$S(k_i) = \frac{\alpha}{2} k_i^{-3} \exp \left[ -1.25 \left( \frac{k_i}{k_p} \right)^{-2} \right] \exp \left\{ \ln \gamma \exp \left[ -\frac{(\sqrt{k_i/k_p} - 1)^2}{2\sigma^2} \right] \right\}$$



Directional spreading function

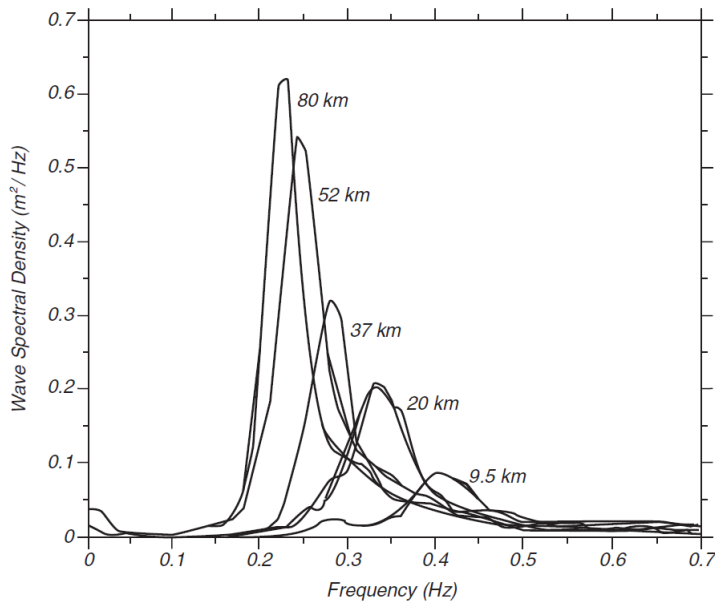
$$D(\theta_j) = \begin{cases} \frac{2}{\pi} \cos^2 \theta_j & |\theta_j| \leq 90^\circ \\ 0 & |\theta_j| > 90^\circ \end{cases}$$



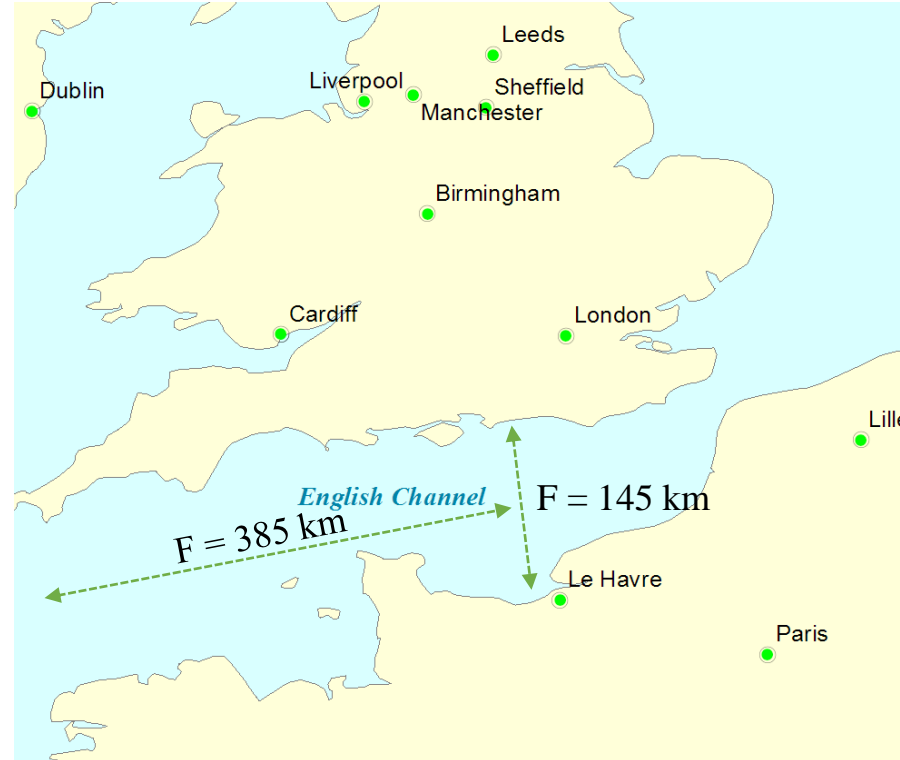
# Sea Surface Modelling – Fetch length

The fetch is a significant factor in the development of wind waves

JONSWAP wave spectrum for different fetches

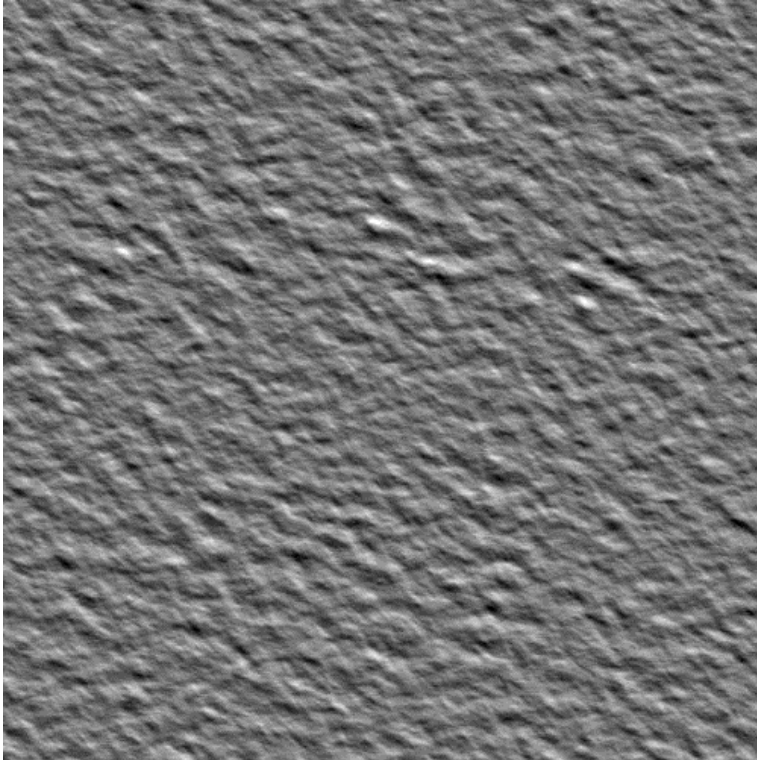


Stewart, R. H. (2008). *Introduction to physical oceanography*.

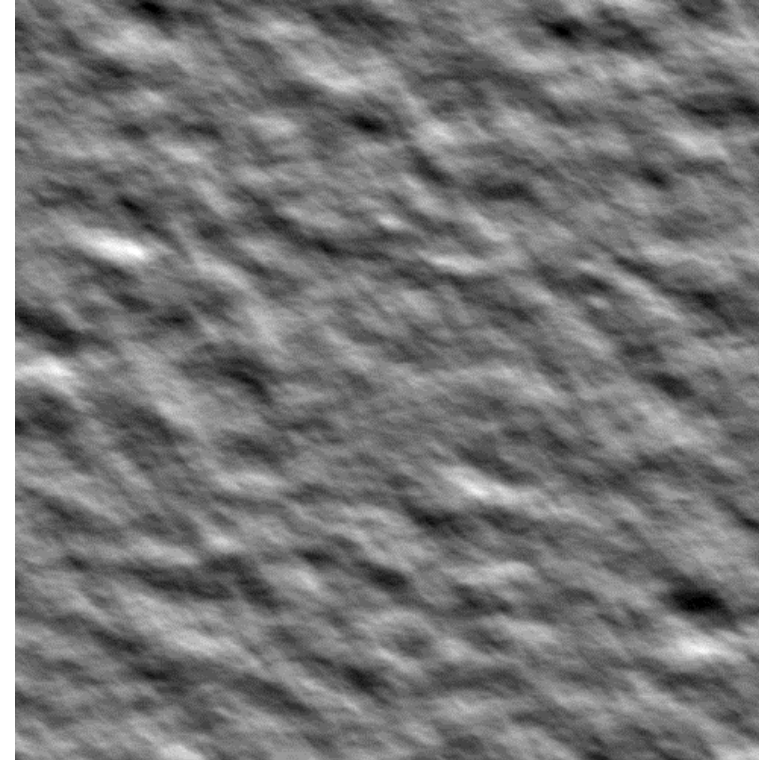


# Sea Surface Modelling – Time domain

$V_w = 7 \text{ m/s}$ ,  $F = 20 \text{ km}$



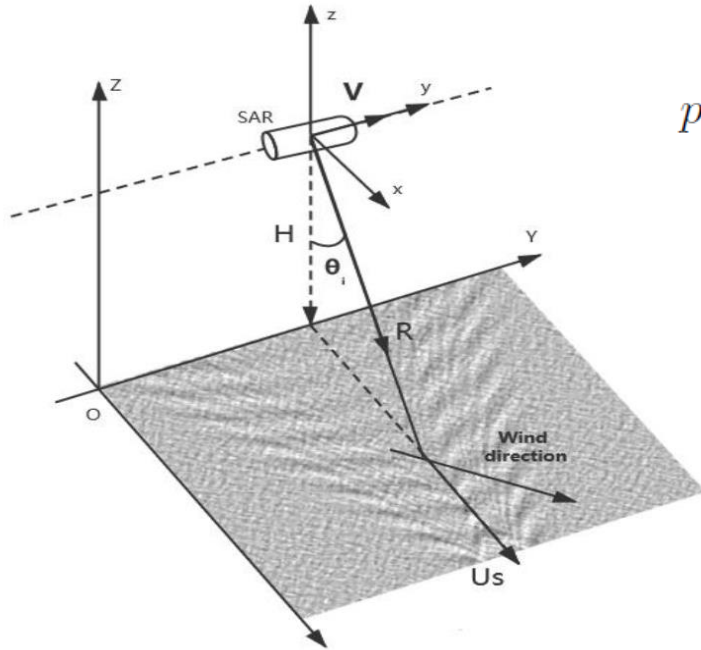
$V_w = 7 \text{ m/s}$ ,  $F = 105 \text{ km}$





# SAR image simulation – velocity bunching of gravity waves

$$I(x, y) = \frac{\pi T_i}{2V} \iint \delta(y - y_0) \frac{\bar{\sigma}(x_0, y_0)}{p_a^1(x_0, y_0)} \times \exp \left\{ -\pi^2 \left[ \frac{x - x_0 - \frac{R}{V} u_r(x_0, y_0)}{p_a^1(x_0, y_0)} \right]^2 \right\} dx_0 dy_0$$



SAR scanning geometry

$$p'_a(x, y) = N_l p_a \left[ 1 + \frac{\pi^2 T_i^4}{N_l^2 \lambda^2} \bar{A}_r(x, y) + \frac{1}{N_l^2} \frac{T_i^2}{\tau_c^2} \right]^{1/2}$$

Degraded azimuthal resolution

$$p_a = \frac{\lambda R}{2VT_i}$$

Single-look azimuthal resolution

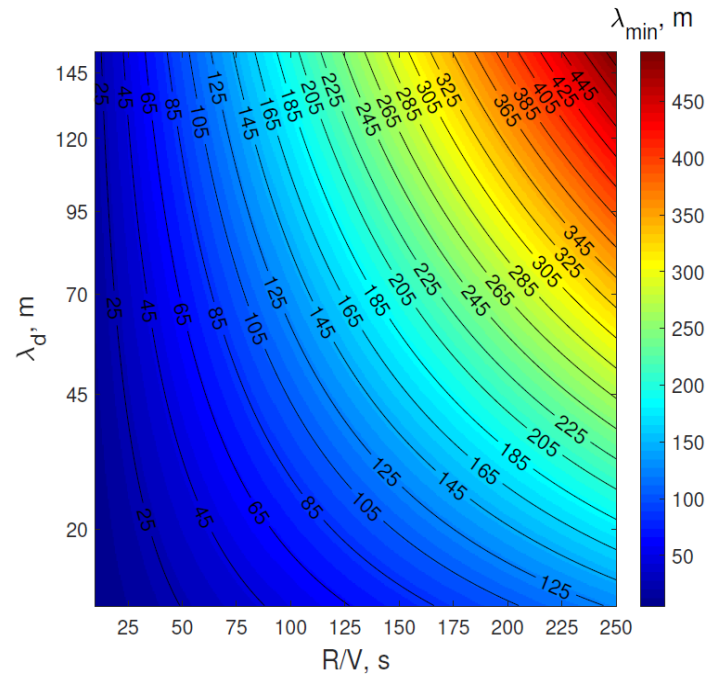
R/V is the range-to-velocity ratio

# SAR simulation

The important limitation of SAR imaging of waves moving in flight direction which is associated with the velocity bunching is the azimuthal cut-off effect.

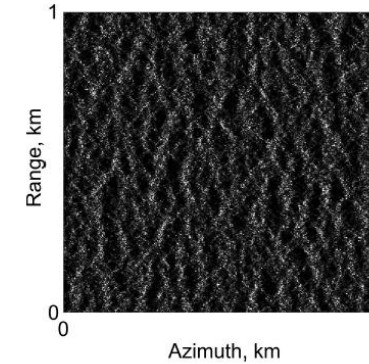
The minimal detectable wavelength of the surface waves can be approximated as

$$\lambda_{\min} = C_0 \frac{R}{V} \sqrt{H_s}$$

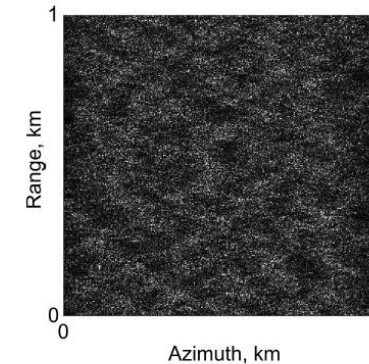


(a)

Simulated SAR images of the sea surface with  $V_w = 10.7$  m/s and  $\lambda_d = 95.5$  m for (b) airborne ( $R/V = 23.1$  s) and (c) satellite ( $R/V = 107.1$  s) platforms.



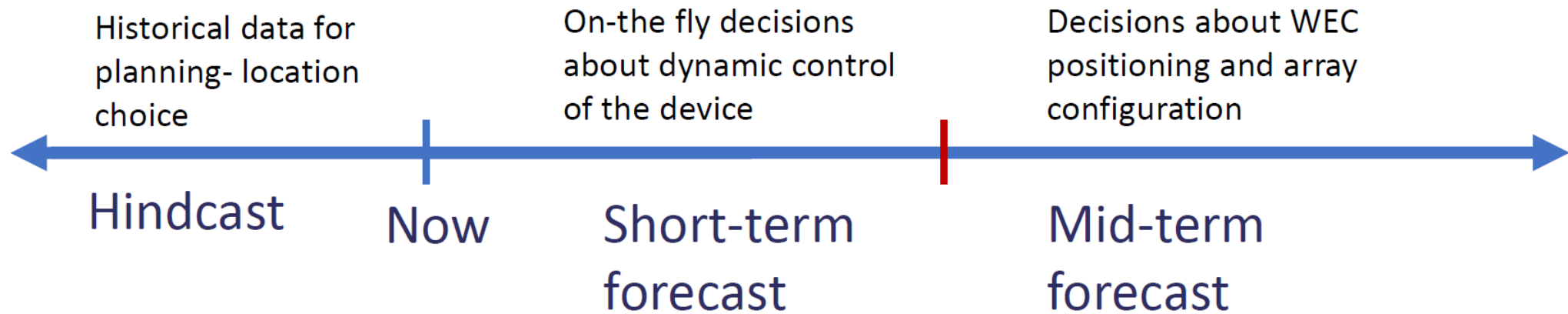
(b)



(c)

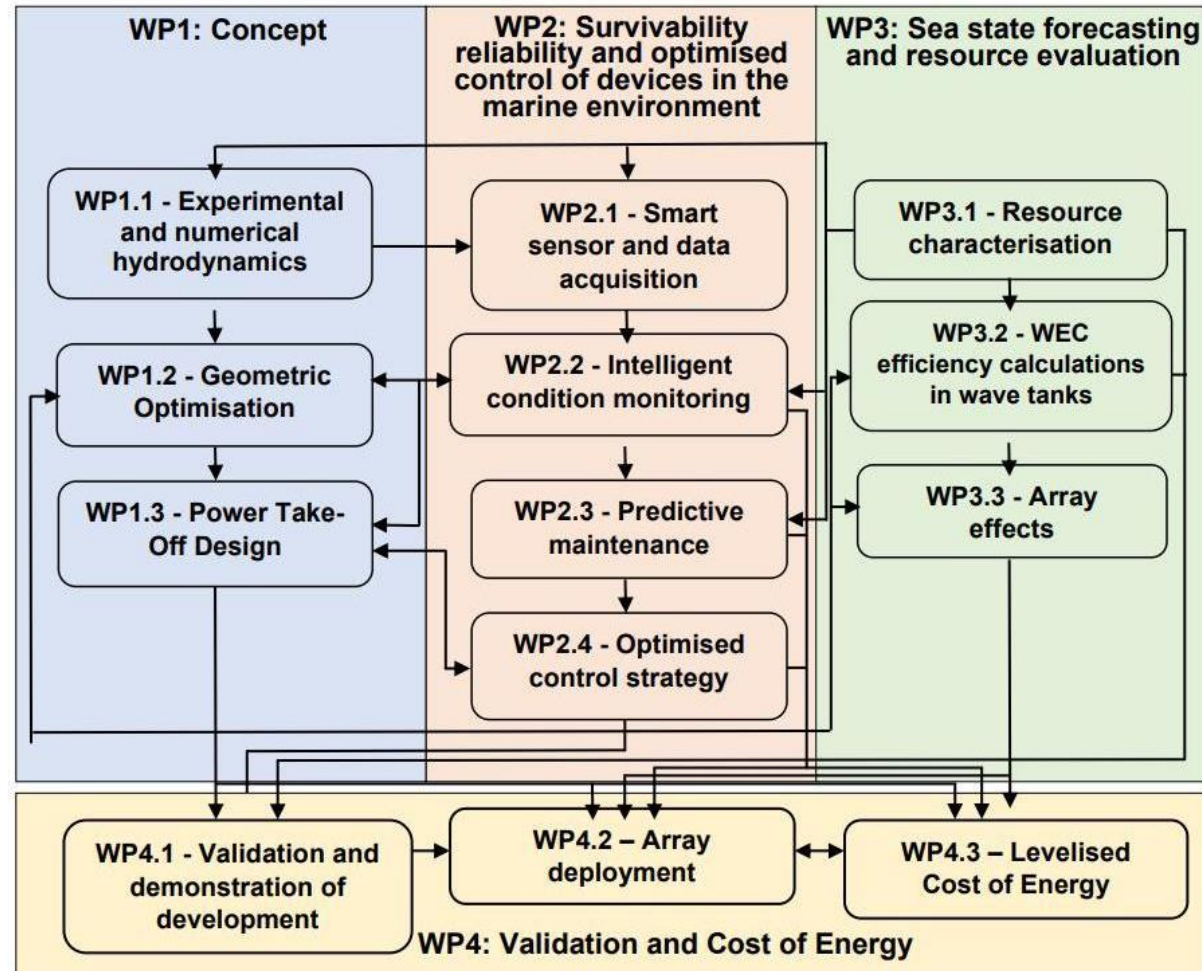
Rizaev, I. G., Karakuş, O., Hogan, S. J., & Achim, A. (2022). Modeling and SAR Imaging of the Sea Surface: a Review of the State-of-the-Art with Simulations. ISPRS Journal of Photogrammetry and Remote Sensing, 187, 120-140.

# Uses of SmartWave



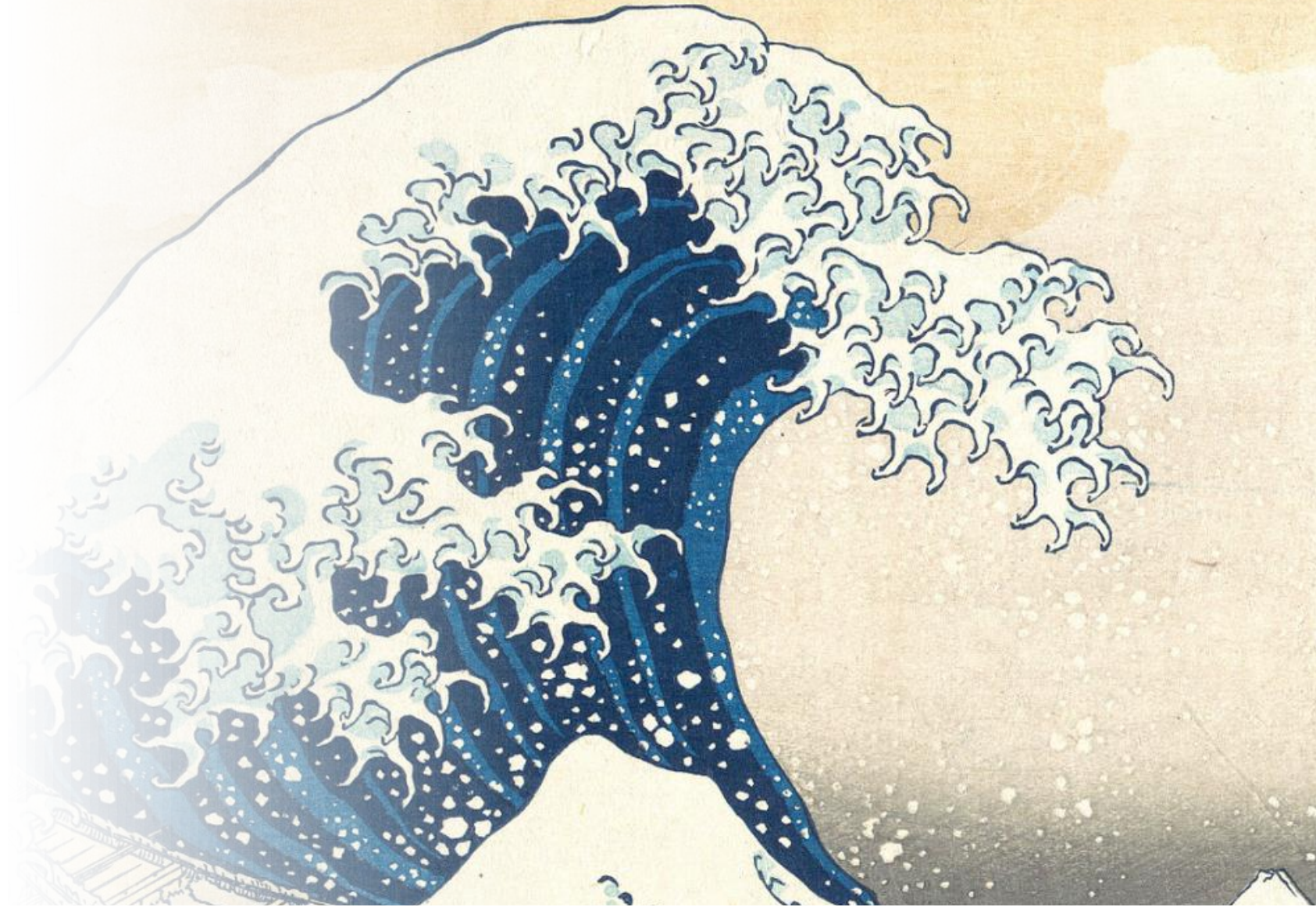


# Interaction with other WPs





# Thank you!



Engineering and  
Physical Sciences  
Research Council



UNIVERSITY OF HULL | ENERGY AND ENVIRONMENT INSTITUTE

